

Orbital correlations in the pseudo-cubic  $O$  and rhombohedral  $R$ -phases of  $\text{LaMnO}_3$ Xiangyun Qiu,<sup>1</sup> Th. Prosen,<sup>2</sup> J. F. Mitchell,<sup>3</sup> and S. J. L. Billinge<sup>1</sup><sup>1</sup>Department of Physics and Astronomy, Michigan State University, E. Lansing, MI 48824<sup>2</sup>Los Alamos National Laboratory, LANSC-E-12, MS H805, Los Alamos, NM, 87545<sup>3</sup>Material Science Division, Argonne National Laboratory, Argonne, IL, 60439

(Dated: November 2, 2021)

The local and intermediate structure of stoichiometric  $\text{LaMnO}_3$  has been studied in the pseudocubic and rhombohedral phases at high temperatures (300 to 1150 K). Neutron powder diffraction data were collected and a combined Rietveld and high real-space resolution atomic pair distribution function analysis carried out. The nature of the Jahn-Teller (JT) transition around 750 K is confirmed to be orbital order to disorder. In the high temperature orthorhombic ( $O$ ) and rhombohedral ( $R$ ) phases the  $\text{MnO}_6$  octahedra are still fully distorted locally. The data suggest the presence of local orbitally ordered clusters of diameter  $\sim 1.6$  Å (four  $\text{MnO}_6$  octahedra) implying strong nearest neighbor JT anti-ferrodistortive coupling.

PACS numbers: 61.12.-q, 75.47.Lx, 75.47.Gk

The perovskite manganites related to  $\text{LaMnO}_3$  continue to yield puzzling and surprising results despite intensive study since the 1950's [1, 2, 3]. The pervading interest comes from the delicate balance between electronic, spin and lattice degrees of freedom coupled with strong electron correlations. Remarkably, controversy still exists about the nature of the undoped end member material,  $\text{LaMnO}_3$ , where every manganese ion has a nominal charge of  $3+$  and no hole doping exists. The ground-state is well understood as an  $A$ -type antiferromagnet with long-range ordered, Jahn-Teller (JT) distorted,  $\text{MnO}_6$  octahedra [4, 5] that have four shorter and two longer bonds [6]. The elongated occupied  $e_g$  orbitals lie down in the  $xy$ -plane and alternate between pointing along  $x$  and  $y$  directions, the so-called  $O^0$  structural phase [4, 5]. At  $T_{JT} \sim 750$  K the sample has a first-order structural phase transition to the  $O$  phase that formally retains the same symmetry but is pseudo-cubic with almost regular  $\text{MnO}_6$  octahedra (six almost equal bond-lengths). In this phase the cooperative JT distortion has essentially disappeared. It is the nature of this  $O$  phase that is unclear. The  $O$ -phase has special importance since it is the phase from which ferromagnetism and colossal magnetoresistance appears at low temperature at Ca, Sr dopings  $> 0.2$  [1, 5].

The additional complication of disorder due to the presence of alkali-earth dopant ions, and the doped-holes on manganese sites, is absent in  $\text{LaMnO}_3$ . However, there is still disagreement about the precise nature of the  $O$ -phase in this simple case. In 1996 Millis [7], based on fits to data of a classical model that included JT and lattice terms, estimated the energy of the JT splitting to be  $\sim 0.4$  eV and possibly as high as  $2.4$  eV. This high energy scale clearly implies that the JT distortions are not destroyed by thermal excitation at 750 K and the  $O^0$ - $O$  transition is an order-disorder transition where local JT octahedra survive but lose their long-range spatial correlations. This picture is supported by some probes sensi-

tive to local structure, for example XAFS [8, 9] and Raman scattering [10], each of which presents evidence that structural distortions consistent with local JT effects survive above  $T_{JT}$ . However while compelling, this picture seems hard to reconcile with the electronic and magnetic properties. In the  $O$ -phase the material's conductivity increases (despite being at higher temperature and more disordered), and becomes rather temperature independent [11, 12], and the ferromagnetic correlations become stronger compared to the  $O^0$ -phase [12, 13]. These results clearly imply greater electronic mobility in the  $O$ -phase, which appears at odds with the persistence of JT distortions above  $T_{JT}$  that are becoming orientationally disordered. The disordering should result in more carrier scattering and higher resistivity, contrary to the observation [12]. Furthermore, a sharp decrease in the unit cell volume at  $T_{JT}$  has been reported [14]. This mimics the behavior observed when electrons delocalize and become mobile at  $T_C$  in the doped materials [15], whereas from geometrical arguments, an orbital disordering of rigid octahedra would result in a volume increase.

We have used a diffraction probe of the local atomic structure, neutron pair distribution function (PDF) analysis, to see if the local and average behaviors can be reconciled and understood. This method allows quantitative structural refinements to be carried out on intermediate length-scales in the nanometer range. We confirm that the JT distortions persist locally at all temperatures, and quantify the amplitude of these local JT distortions. No local structural study exists of the high-temperature rhombohedral  $R$ -phase that exists above  $T_R = 1010$  K. We show for the first time that even in this phase where the octahedra are constrained by symmetry to be undistorted, the local JT splitting persists. Fits of the PDF over different  $r$ -ranges indicate that locally distorted domains have a diameter of  $\sim 1.6$  Å with about four  $\text{MnO}_6$  octahedra spanning the locally ordered cluster. We show that the crystallographically observed volume reduction

at  $T_{JT}$  [14] is consistent with increased octahedral rotational degrees of freedom and is not the reduction in  $MnO_6$  observed crystallographically. We speculate that nanoclusters of the low- $T$  structure form on cooling at  $T_R$  but are disordered and align themselves along the three crystal axes. These domains grow, and the orbital ordering pattern becomes long-range ordered below  $T_{JT}$ .

Powder samples of 6 g were prepared from high purity  $MnO_2$  and  $La_2O_3$ ; the latter was pre-reduced at 1000 °C to remove moisture and carbon dioxide. Final firing conditions were chosen to optimize the oxygen stoichiometry at 3.00. The crystallographic behavior was confirmed by Rietveld refinements using program GSAS [16]. Both the differential thermal analysis (DTA) and Rietveld measurements estimated the same phase transition temperatures of  $T_{JT} = 735$  K and  $T_R = 1010$  K. These values indicate that the sample is highly stoichiometric [4, 17]. Neutron powder diffraction data were collected on the NPDF diffractometer at the Lujan Center at Los Alamos National Laboratory. The sample, sealed in a cylindrical vanadium tube, was measured from 300 to 1150 K. After temperature cycling, a further measurement at 300 K confirmed that the sample was unchanged by the thermal cycling in reducing atmosphere. Data reduction to obtain the PDFs [18] was carried out using program PDFgetN [19]. PDF modeling was carried out using the program PDFFIT [20].

We first confirm the earlier XAFS results [8, 9] and establish that in the  $O^0$ -phase the full JT distortion persists in the local structure. This result can be seen qualitatively in Fig. 1. In panel (a) the first peak in the PDF, coming from Mn-O nearest neighbor (nn) bonds, is shown. This peak is upside-down because of the negative neutron scattering length of Mn [18]. It is double-valued because of the presence of short-bonds of average length 1.94 Å, and long-bonds of length 2.16 Å, coming from the JT distorted octahedra. The doublet is clearly evident at low temperature below  $T_{JT}$ . However, the splitting persists up to the highest temperature and remains larger than the thermal broadening of the peaks. This shows qualitatively and intuitively that the JT distortion survives at all temperatures. The peaks do broaden at higher temperature due to increased thermal motion [18] and the two contributions to the doublet are not resolved at high temperature. However, it is clear that the peak is not a broad, single-valued, Gaussian at high temperature as predicted from the crystallographic models.

We would like to see if there is any change in the peak profile on crossing the  $T_{JT}$  beyond normal thermal broadening. To test this we plot the change in this nn Mn-O peak between  $T = 720$  K and  $T = 880$  K, as it crosses  $T_{JT}$ , and compare this to the change in the peak on going from 650 K to 720 K. The latter case has approximately the same temperature differential (thermal broadening will be comparable) but there is no structural transition in that range. The difference curves from these two sit-

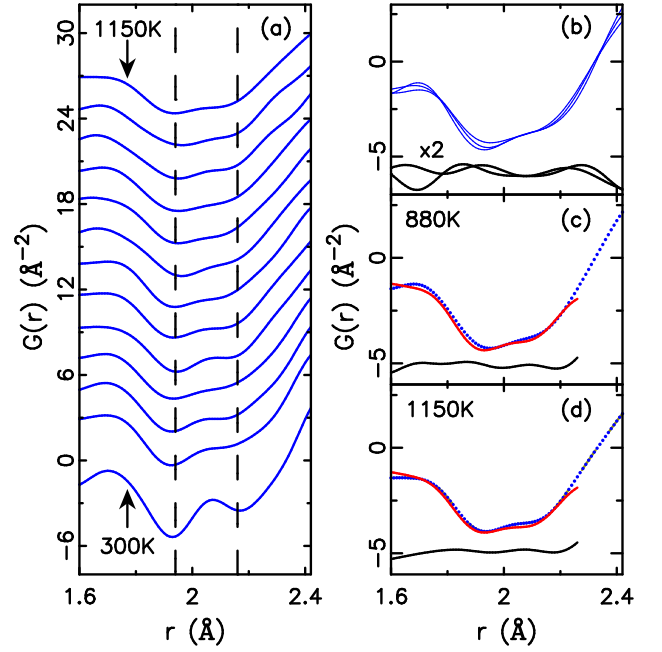


FIG. 1: (a) Low- $r$  region of the experimental PDFs at all temperatures of interest along the y axis with increasing temperature. Two dashed lines indicate the Mn-O short and long bonds at 1.94 and 2.16 Å, respectively. (b) PDFs at 650, 720, and 880 K without offset. The differences between 720 and both 650 K and 880 K (both high T minus low T) are shown offset below. (c) Two-Gaussian fit of PDF data at 880 K (solid dots). Solid line denotes fitted curve with the difference curve offset below. (d) Same as (c) for 1150 K PDF data.

uations, shown in Fig. 1(b), are almost identical. We conclude that there is virtually no change to the  $MnO_6$  octahedra as they go from the  $O^0$  to the  $O^+$  phase.

Finally, to quantify the nature of the local JT distortions, we have fit two Gaussian peaks to the nearest-neighbor  $MnO_6$  doublet in the experimental data at all temperatures. The quality of the fits at "low" (880 K) and high (1150 K) temperature are rather good, as can be seen in Fig. 1(c) and (d). The position and width of each peak, and the total integrated intensity of the doublet, were allowed to vary (the intensities of the long and short bond distributions were constrained to be 1:2 in the fits). The weighted residual factor  $R_{wp}$  varies from 1% at high temperature to 5% at low temperature indicating excellent agreement over all temperatures. Attempts to fit a single Gaussian in the  $O^+$  phase resulted in significantly worse agreements. The results of the temperature-dependent fits are shown in Fig. 2. No anomaly of any kind can be identified across the  $T_{JT} = 735$  K. The integrated intensities and peak positions do not change significantly with temperature from 300 K to 1150 K indicating that the average bond-lengths of the short- and long-bonds in the JT distorted octahedra are rather temperature independent. The peak widths increase slightly with temperature due to increased thermal motion (Fig. 2(b));

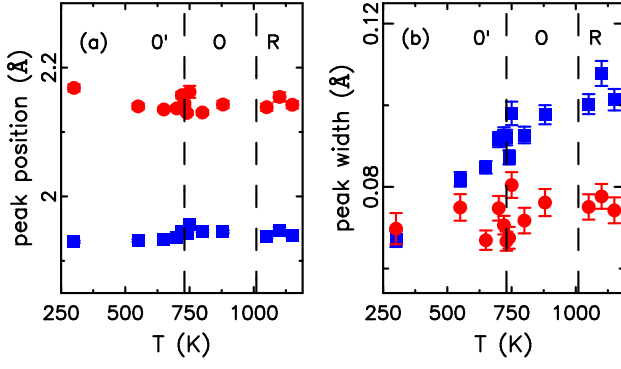


FIG. 2: Fitting results of the Mn-O PDF peaks with two-Gaussians: the low-r peak ( ) around 1.94 Å, and the high-r peak ( ) 2.16 Å. The dashed lines denote the phase transition temperatures. (a) Peak positions. (b) Peak widths.

however, there is no clear discontinuity in the peak broadening associated with the phase transition. The results confirm that the local JT distortions persist, virtually unstrained, into the O and R-phases.

Fits to the nearest neighbor Mn-O peaks show a large JT distortion in the O-phase, whereas crystallographically the  $\text{MnO}_6$  octahedra are almost regular (six equal bonds). This implies that the average structure results from a loss of coherence of the ordering of the JT distorted octahedra and that the JT transition is an orbital order-disorder transition. In principle we can test the extent of any orbital short-range-order in the PDF by fitting models to the data over different ranges of  $r$ . Fits confined to the low-r region will yield the local (JT distorted) structure whereas fits over wider ranges of  $r$  will gradually cross over to the average crystallographic structure. To extract the size of the short-range ordered clusters, we have fit the PDF from  $r_{\text{min}} = 1.5$  Å to  $r_{\text{max}}$ , where  $r_{\text{max}}$  was increased step by step from 5 Å to 20 Å, by which time the PDF refinement agrees with the average structure refinement from Rietveld. This was done for all data-sets. The model used at all temperatures was the low-temperature structure in the Pbnm space group. Representative results are shown in Fig. 3. Note that three distinct bond-lengths are obtained from modeling although only two peaks can be resolved directly in the PDF at low-r. The amplitude of the refined JT distortion is constant as a function of  $r_{\text{max}}$  at 300 K reflecting the fact the orbital order is perfectly long-range. Regardless of the range fit over, the full JT distortion is recovered (Fig. 3 (a)). At higher temperature, and especially in the O phase the amplitude of the refined distortion falls off smoothly as the fit range is extended to higher-r, until it asymptotically approaches the much smaller crystallographically refined value. We understand this behavior in the following way. Domains of local orbital order exist in the O phase. These may resemble the pattern of orbital order at low-temperature ( $O^0$  phase), and for

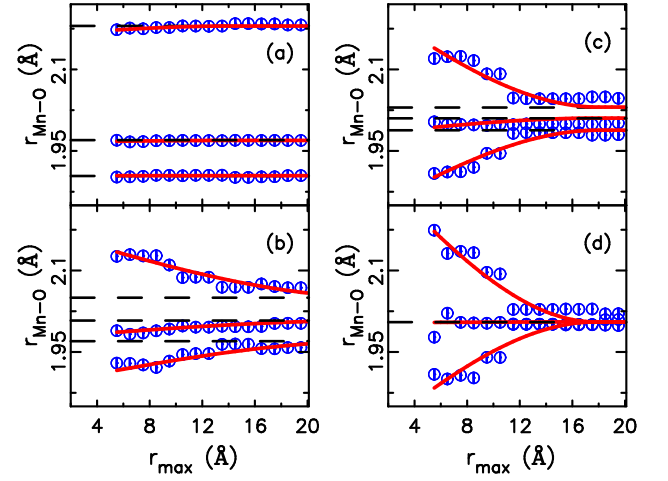


FIG. 3: Mn-O bond lengths from the refined structure model as a function of  $r_{\text{max}}$  are shown as circles. Error bars are smaller than, but comparable, to the symbol size. The solid red lines are the expected behavior assuming spherical locally ordered clusters. All three bond lengths are self-consistently fit with a single parameter, the cluster size. The horizontal dashed lines indicate the Mn-O bond lengths from Rietveld refinements. (a) 300 K, (b) 740 K, (c) 800 K, (d) 1100 K.

convenience this is how we have modeled them. These domains do not propagate over long-range and are orientationally disordered in such a way that, on average, the observed pseudo-cubic structure is recovered. We can estimate the domain size by assuming that the orbitals are ordered inside the domain but uncorrelated from one domain to the neighboring domain. This results in a fall-off in the amplitude of the refined distortion with increasing fit range with a well-defined PDF form-factor [1], assuming spherical domains, that depends only on the diameter of the domain. The three curves of refined-bond-length vs.  $r_{\text{max}}$  from the short, medium and long bonds of the  $\text{MnO}_6$  octahedron could be fit at each temperature with the diameter of the domain as the one single parameter. Representative fits are shown in Fig. 3 as the filled circles. The temperature dependence of the inverse domain diameter is shown in Fig. 4 (a). We find that in the pseudo-cubic O-phase these clusters have a diameter of  $\sim 16$  Å, roughly independent of temperature except close to  $T_{\text{JT}}$  where the size grows. Below  $T_{\text{JT}}$  the correlation length of the order is much greater, although some precursor effects are evident just below  $T_{\text{JT}}$ . The refined domain size of orbital order is similar in the R-phase though the quality of the fits becomes worse in this region. This may be because the nature of the short-range orbital correlations changes, i.e., becomes different from the  $O^0$  phase. The correlation length scale of 16 Å spans over four  $\text{MnO}_6$  octahedra, suggesting strong nearest neighbor JT antiferrodistortive coupling (as expected from the fact that neighboring  $\text{MnO}_6$  octahedra share one oxygen atom) and weak second and higher nn

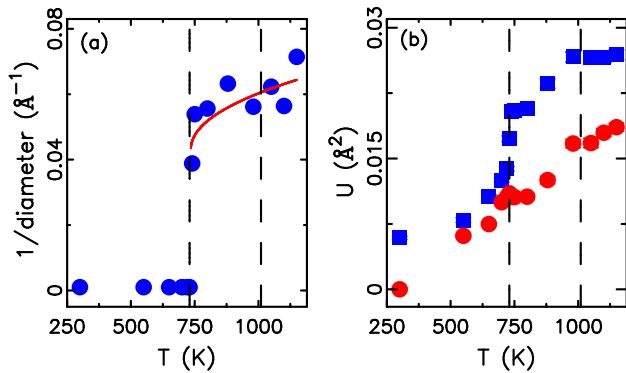


FIG. 4: (a) Inverse of the domain diameter obtained from the fits shown in Fig. 3. Solid is a simple exponential critical curve as a guide to the eye. (b) Thermal displacement parameters of oxygen atoms parallel (blue) and perpendicular (red) to Mn-O bonding directions. The perpendicular component is shift down by  $0.007 \text{ \AA}^2$  for clarity.

coupling.

We now address the issue of the unit-cell volume collapse observed crystallographically [14] and seen in our Rietveld and wide-range PDF refinements. Our Rietveld refinements show that the average Mn-O bond length  $\langle r_{\text{Mn-O}} \rangle$  contracts across the transition resulting a volume collapse of the  $\text{MnO}_6$  octahedron, which is found to fully account for the unit cell volume reduction. In the absence of local structural information to the contrary, this behavior is most readily explained if charges are delocalizing resulting in more regular  $\text{MnO}_6$  octahedra and a smaller unit cell, as observed at higher doping in the  $\text{La}_{1-x}\text{Ca}_x\text{MnO}_3$  system [22]. However, we have clearly shown that locally the  $\text{MnO}_6$  octahedra do not change their shape and the local  $r_{\text{Mn-O}}$  is independent of temperature. The volume collapse must therefore have another physical origin. The most likely scenario is an increase in octahedral tilting amplitude. This is similar to the behavior seen at the pseudo-cubic transition of perovskite  $\text{AlF}_3$  [23]. If the increased tilting is not long-range ordered a response is expected in oxygen displacement parameters perpendicular to the Mn-O bond. These are shown in Fig. 4 (b) as the circles. The temperature dependence indicates that this motion is rather soft ( $U$  increases strongly with temperature) but there is no clear discontinuity at  $T_{\text{JT}}$ . However, the change in tilt amplitude required to explain the volume collapse is tiny. The average tilt angle needs to increase only by 0.4 degrees to account for the observed 0.38 % volume collapse, which is equivalent to displacing the oxygen atom by only  $0.014 \text{ \AA}$ , thus we may not expect to see a discontinuity in  $U$ .

A large discontinuity in the oxygen displacement parameter parallel to the Mn-O bond is observed in the refinements (Fig. 4 (b) squares). This is precisely what would be expected from a system with JT-distorted octahedra that are orientationally disordered on average.

The sudden increase of conductivity across the JT transition [11, 12] cannot be easily explained by the locally JT distorted  $\text{MnO}_6$  octahedra and increased octahedral tilt in the high temperature phase. We speculate that this conductivity anomaly comes along with the dynamic nature of the JT distortions. Zhou and Goodenough have proposed a vibronic model where some  $\text{Mn}^{3+}$  ions charge disproportionate into  $\text{Mn}^{2+}$  and  $\text{Mn}^{4+}$  [12]. We see no direct evidence for this charge disproportionation but if it occurs on a small minority of sites it would be undetectable in our data.

To summarize, the PDF clearly shows that the JT transition in  $\text{LaMnO}_3$  is of orbital order-disorder type; however, 16 Å nanoclusters of short-range orbital order persist in the high temperature O and R-phases. Our analysis of the PDF shows that this is a promising approach to extract nanocluster information in the absence of single crystal diffraction data.

Work at MSU was supported by NSF through grant DMR-0304391. Work at ANL was supported by DOE under Contract No. W-31-109-ENG-38. Beam time on NPDF at Lujan Center was funded by DOE through contract W-7405-ENG-36.

- 
- [1] A. P. Ramirez, J. Phys. Condens. Matter 9, 8171 (1997).
  - [2] M. B. Salamon et al., Rev. Mod. Phys. 73, 583 (2001).
  - [3] E. Dagotto et al., Nanoscale Phase Separation and Colossal Magnetoresistance, Springer-Verlag, Amsterdam, 2003.
  - [4] J. Rodriguez-Carvajal et al., Phys. Rev. B 57, R3189 (1998).
  - [5] E. O. Wollan et al., Phys. Rev. 100, 545 (1955).
  - [6] Th. Proffen et al., Phys. Rev. B 60, 9973 (1999).
  - [7] A. J. Millis, Phys. Rev. B 53, 8434 (1996).
  - [8] M. C. Sanchez et al., Phys. Rev. Lett. 90, 045503 (2003).
  - [9] E. A. Ruyter et al., J. Magn. Magn. Mater. 233, 88 (2001).
  - [10] E. G. Ranado et al., Phys. Rev. B 62, 11304 (2001).
  - [11] P. Mandal et al., Phys. Rev. B 64, 180405 (2001).
  - [12] J.-S. Zhou and J. B. Goodenough, Phys. Rev. B 60, R15002 (1999). Phys. Rev. B 68, 144406 (2003).
  - [13] M. Tovar et al., Phys. Rev. B 60, 10199 (1999).
  - [14] T. Chatterji et al., Phys. Rev. B 68, 052406 (2003).
  - [15] P. G. Radaelli et al., Phys. Rev. B 56, 8265 (1997).
  - [16] A. C. Larson and R. B. Von Dreele, GSAS Report No. LAUR-86-748, Los Alamos National Laboratory, 1987.
  - [17] P. Norby et al., J. Solid State Chem. 119, 191 (1995).
  - [18] T. Egami and S. J. L. Billinge, Underneath the Bragg Peaks: Structural analysis of complex materials, Pergamon Press, Elsevier, Oxford, England, 2003.
  - [19] P. F. Peterson et al., J. Appl. Crystallogr. 33, 1192 (2000).
  - [20] Th. Proffen et al., J. Appl. Crystallogr. 32, 572 (1999).
  - [21] X. Qiu and S. J. L. Billinge, (2004), unpublished.
  - [22] S. J. L. Billinge et al., Phys. Rev. Lett. 77, 715 (1996).
  - [23] P. J. Chupas et al., J. Am. Chem. Soc. 126, 4756 (2004).